Fusion Engineering and Design 109–111 (2016) 1193–1198

Contents lists available at ScienceDirect

Fusion Engineering and Design

journal homepage: www.elsevier.com/locate/fusengdes

Study on thermal mixing of liquid–metal free-surface flow by obstacles installed at the bottom of a channel

Koji Kusumi[a], Tomoaki Kunugi[a,*], Takehiko Yokomine[a], Zensaku Kawara[a], Jesus A. Hinojosa[b], Egemen Kolemen[b], Hantao Ji[b], Erik Gilson[b]

[a] Department of Nuclear Engineering, Kyoto University, C3-d2S06, Kyoto-Daigaku Katsura, Nishikyo-Ku, Kyoto 615-8540, Japan
[b] Princeton Plasma Physics Laboratory, 100 Stellarator Rd., Princeton, NJ 08540, USA

HIGHLIGHTS

- Experiments of thermal mixing in liquid metal film-flow by obstacles were performed.
- Delta-wing obstacle showed good thermal mixing performance.

ARTICLE INFO

Article history:
Received 1 September 2015
Received in revised form
22 December 2015
Accepted 24 December 2015
Available online 9 January 2016

Keywords:
Experiment
Liquid metal
Free-surface
Obstacles
Thermal mixing

ABSTRACT

One of the key challenges of the liquid divertor concepts in fusion reactors is the heat removal from the surface of liquid metal film-flow to the bottom wall, because thermal radiation and particle fluxes from the fusion core are deposited on the free-surface. This study investigates the possibility of the enhancement of heat removal by using various obstacles installed at the bottom of the liquid metal free-surface flow. Cubic and delta-wing obstacles are examined in this study. The obstacles installed at the center of the flow channel, upstream of the free-surface heat source. The experiments were conducted in the range of *Re* from 2000 to 18,000 under constant heating. The temperature on the bottom wall increased with increase of flow rate. The delta-wing obstacle showed the better thermal performance compared to the cubic obstacle and without obstacle case. Since the delta-wing obstacle generated the strong vortex with increasing *Re*, thermal mixing of liquid-film enhanced, and eventually led to highly localized heat fluxes at the bottom wall. Therefore, it is possible to remove the high heat flux locally from the wall.

1. Introduction

The liquid divertor concepts in fusion reactors have been widely investigated for magnetic fusion reactors, such as Abdou [1], Kunugi [2,3], Mirnov [4], Jaworski [5].

Recently, Rhoad [6] investigated the effects of magnetic field on the turbulent wake of a cylinder in free-surface MHD channel flow. He reported that the MHD flow under the vertical magnetic field showed the best performance for heat transfer enhancement in the range of the interaction parameter, *N*, from 0 to 1. To our knowledge, only a few experimental studies on heat transfer of the free-surface flow have conducted. Mück [7] numerically studied the characteristics of Magneto-Hydro-Dynamics (MHD) flow and heat transfer and reported the strong influence of the magnetic field such as the vortices elongated and aligned with parallel magnetic field. Chatterjee [8] and Huang [9] numerically investigated the fluid mixing effect by installing obstacles in the MHD channel flow. Huang [9] also studied heat transfer performance by installing hemispherical obstacles in MHD free-surface flow. Their results show that higher height obstacles and lower Hartmann number condition increases heat transfer performance. On the other hand, heat transfer of delta-wing obstacle in air and hydrodynamic flow, as opposed to liquid metals, was studied by many researchers including Gentry [10] and Joardar [11]. The delta-wing vortex generators allow easy generation of long vortex structures that are parallel to flow direction. Therefore, it expected that the vortex generated by the delta-wing obstacle will strongly interact with the vertical and transverse magnetic fields.

In this study, the delta-wing and the cubic obstacle were used as the vortex generators, and their wake effects on thermal mixing in liquid metal ($Ga_{67}In_{20.5}Sn_{12.5}$) free-surface flow were investigated. In order to grasp the thermal mixing of these obstacles, the liquid metal free-surface flow in the channel without magnetic field was

* Corresponding author. Tel.: +81 75 7535823.
E-mail address: kunugi@nucleng.kyoto-u.ac.jp (T. Kunugi).

http://dx.doi.org/10.1016/j.fusengdes.2015.12.055
0920-3796/

Nomenclature

A	area of channel cross section [m^{-2}]
d	width of obstacle [m]
H	flow height [m]
h	heat transfer coefficient [$W\,m^{-2}\,K^{-1}$]
L	length of channel [m]
l	characteristic length ($l = 4A/(W + 2H)$) [m]
N	interaction parameter [−]
Q	total energy [W]
Q_{in}	input power [W]
q_w	heat flux from wall [$W\,m^{-2}$]
Re	Reynolds number [−]
T_b	bulk fluid temperature [°C]
T_{in}	inlet temperature [°C]
T_{out}	outlet temperature [°C]
T_{TC}	thermocouple temperature at wall [°C]
u	flow velocity [ms^{-1}]
W	width of channel [m]
β	blockage ratio [−]
θ	lift angle from bottom of the channel [°]
φ	apex angle [°]

partially heated and the temperature distributions on the channel bottom were measured.

2. Experiments

An experimental apparatus used in this study is called "LMX (Liquid Metal Experiment)" located at Princeton Plasma Physics Laboratory (PPPL).

2.1. Experimental apparatus

The LMX consists of 0.80 m length, 0.10 m width acrylic channel as a test section, a vortex flow meter, an Archimedes-style screw pump, a heat exchanger cooled by a de-ionized water and a storage tank as illustrated in Fig. 1. The working fluid was a gallium–indium–tin ($Ga_{67}In_{20.5}Sn_{12.5}$) eutectic alloy described in Table 1 that flowed through the channel with a mean depth of 0.01 m at the flow velocities from 0.03 to 0.20 ms^{-1}. Argon gas as a pressurized gas was used to prevent the oxidation. 25 K-type thermocouples with the accuracy of ±0.1°C were installed at the bottom wall of channel with mostly equi-spaced separation of 0.034 m as illustrated in Fig. 2. In order to calculate the heat loss and the mean

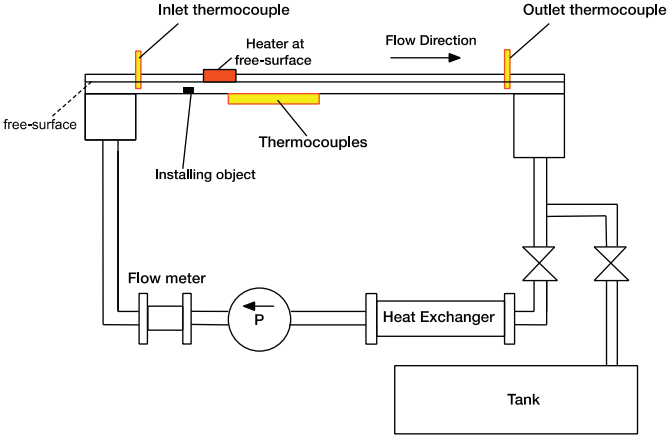

Fig. 1. Experimental apparatus.

Table 1
Physical Properties of $Ga_{67}In_{20.5}Sn_{12.5}$ alloy (room temperature) [12].

Parameters	Symbols	Value
Density [$kg\,m^{-3}$]	ρ	6360
Viscosity [$m^2\,s^{-1}$]	υ	2.98×10^{-7}
Melting point [°C]	T_{melt}	10.5
Boiling point [°C]	$T_{boiling}$	1300
Thermal conductivity [$W\,m^{-1}\,K^{-1}$]	k	16.5
Specific heat [−]	c_p	365

temperature gradient of the flow for the heat flux evaluation, the K-type thermocouples were installed inside the fluid at the inlet and outlet positions of the channel, respectively. The test obstacle was installed at the center of the flow channel and at the upstream of the heater position installed at the free-surface as a black rectangular shown in Fig. 2. The obstacles blockage ratio ($\beta = d/2L$; d is the width of obstacle and $2L$ is the width of the channel) is roughly 0.05. The experiments were performed Reynolds number range of 3000 to 18,000, based on the equivalent hydraulic diameter and the mean flow velocity. The fluid circulated using an Archimedes-style screw pump with a constant flow rate with 5% flow fluctuation around the mean as described in [6]. The heater plate made of Aluminum Nitride ceramic has an area of 0.075 m × 0.025 m is placed on the free-surface. This heater injects a constant heat flux of 0.18 $MW\,m^{-2}$ to the fluid and raised the surface temperature of flow by a few degrees. A heat exchanger installed behind the pump used to cool the heated fluid back to starting temperature.

2.2. Vortex generators

The experiments were conducted for three different configurations: (1) no obstacle, (2) cubic obstacle, and (3) delta-wing obstacle. The size of the cubic obstacle was designed such that the blockage ratio is 0.05. The delta-wing obstacle has 2 characteristic angles: a lift angle of $\theta = 20°$ from the bottom wall of the channel and an apex angle of $\phi = 25°$. This delta-wing configuration is illustrated in Fig. 3. Both of the obstacles were made of acrylic resin.

3. Heat flux calculations

The temperature data is measured at the channel bottom wall as well as at the channel inlet and outlet. The heat flux, q_w, at the bottom wall is defined as

$$q_w(x) = h\Delta T(x), \tag{1}$$

where h is overall heat transfer coefficient and $\Delta T(x)$ is the temperature difference between the wall temperature at the thermocouple position x and the bulk temperature. The bulk temperature is assumed as a linear and thus can be calculated from the following formula:

$$T_b(x) = \frac{T_{out} - T_{in}}{L}x + T_{in}. \tag{2}$$

In Eq. (2), T_{in} is the mean temperature at the location of the inlet thermocouple and T_{out} is the temperature at the outlet thermocouple position. L is the distance between the inlet and outlet thermocouples. The energy balance equation to evaluate the heat loss along the channel can be written as,

$$Q = \rho u A c_p (T_{out} - T_{in}), \tag{3}$$

where ρ is density of the fluid, u is the mean velocity, A is the cross-section area of the flow perpendicular to the stream direction. The heat loss, Q_{loss}, can be calculated from Eq. (3) by defining

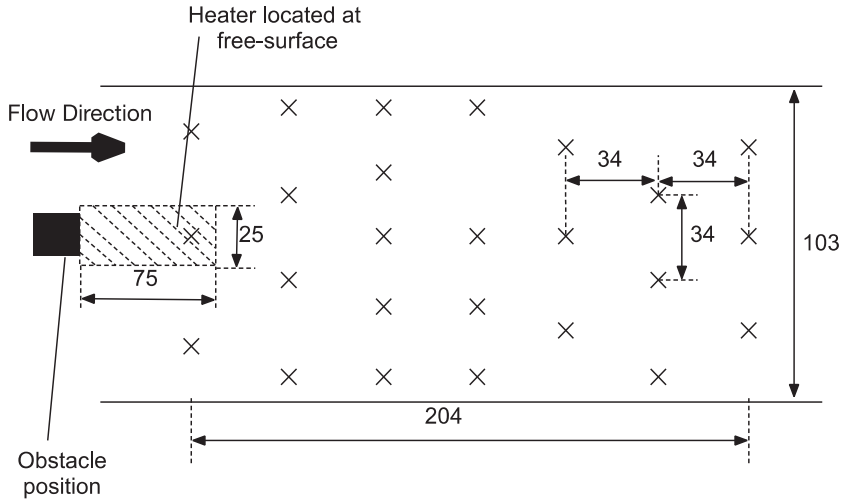

Fig. 2. Schematic of heater location and thermocouples mapping on bottom side (all dimensions are millimeter; *x*-marks are indicating thermocouples locations).

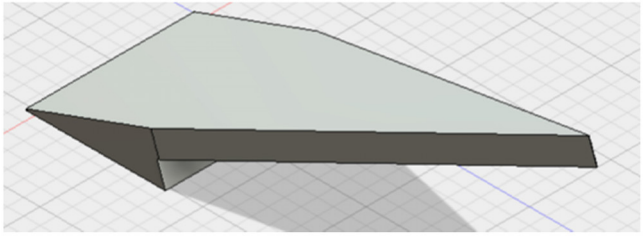

(a) Whole view of delta-wing

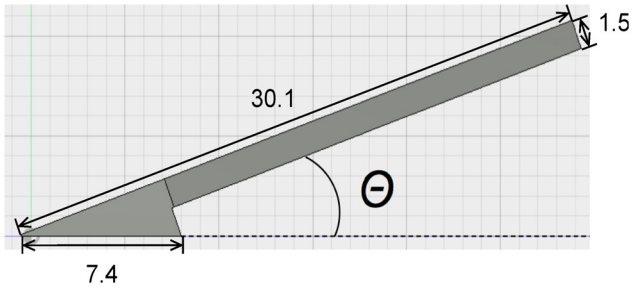

(b) Cross-section view of delta-wing

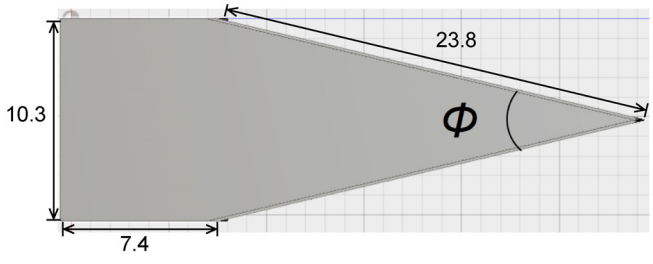

(c) Upper-view of delta-wing

Fig. 3. Delta-wing configuration: (a) whole view of delta-wing, (b) cross-section view of delta-wing and (c) upper-view of delta-wing.

$Q_{loss} = Q_{in} - Q$ where Q_{in} is the heater input power. The local heat flux can be calculated from the Fourier's law as follows:

$$q_w(x) = -k\frac{2\Delta T(x)}{H}, \quad (4)$$

where k is thermal conductivity of the fluid and H is the depth of the fluid. Eq. (4) means that the direction of heat flux was defined as the wall to the bulk fluid.

4. Results and discussion

Fig. 4 shows the temperature contours of low and high *Re* flows without obstacle. These considered as the reference cases. The temperature contours for *Re* = 2400 are rather compact compared to the case of *Re* = 12,000. In the lower *Re* range, the percentage heat loss was high and reduced with *Re*: 59% and 48% for *Re* = 2400 and *Re* = 5000, respectively. In contrast, in the higher *Re* range, the heat loss was lower than low *Re* range: 8.4% and 4.2% for *Re* = 12,000 and 18,000, respectively. It is difficult to discuss on the thermal characteristics of the flow with more than 10% heat loss. Thus, in this paper we will focus on only at the higher *Re* cases with the heat loss of less than 10%.

Fig. 5 shows the temperature contours at higher *Re* cases with cubic and delta-wing obstacles. The higher temperature area in case of the delta-wing obstacle is more elongated in the stream direction than the reference case shown in Fig. 4(b) *Re* = 12,000 and the cubic obstacle case. This means the delta-wing obstacle could transport the high temperature fluid heated at the free-surface to the bottom wall more efficiently than the cubic obstacle and the reference case.

Fig. 6 shows the heat flux vector contours for the reference case (without obstacle) and the cubic obstacle case at *Re* = 18,000. The minus heat flux means the bulk temperature is higher than the wall temperature. This is due to transport of the higher temperature fluid at the free-surface to the wall. The maximum heat fluxes occur at the areas are at the centerline of the wall along the stream direction at *Re* = 18,000 and have heat flux of: $|q_w| = 800$ for the reference case, $|q_w| = 800$ for the cubic obstacle case and $|q_w| = 4800$ for the delta-wing obstacle case. Therefore, it is concluded that obstacle enhances the thermal mixing based on the evaluation of wall heat flux.

The normalized location of the maximum heat flux is measured as, $x/H = 4.46$ for the reference case, $x/d = 12.9$ for the cubic obstacle case, and $x/d = 6.64$ for the delta-wing obstacle case, where d is the equivalent diameter based on the projection area of the obstacle. Thus, it is observed that the delta-wing obstacle enhances the transport of the higher temperature fluid from the free-surface to the wall more than the cubic obstacle.

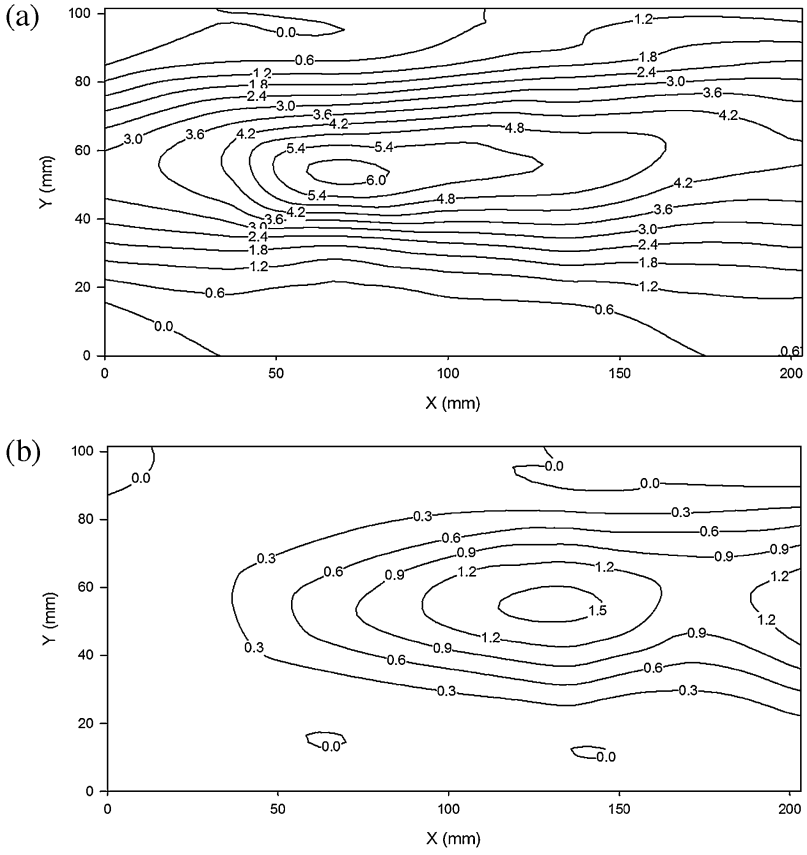

Fig. 4. Temperature contours of low and high *Re* flows without obstacle: *Re* = 2400, (b) *Re* = 12,000.

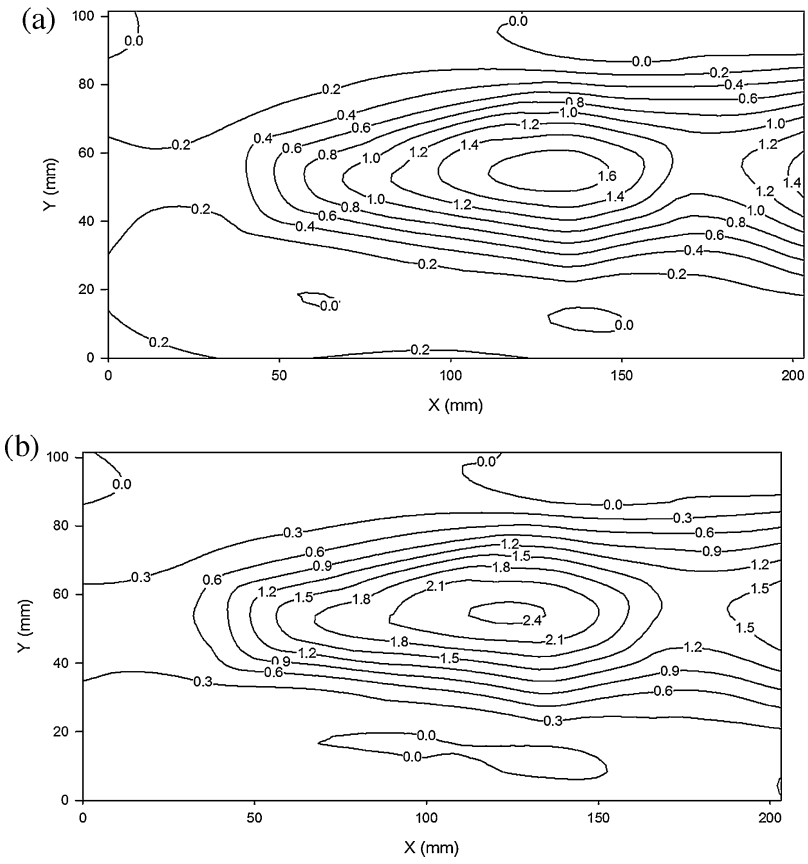

Fig. 5. Temperature contours at higher *Re* cases with cubic and delta-wing obstacles: (a) Cubic obstacle at *Re* = 12,000, (b) Delta-wing obstacle at *Re* = 11,500.

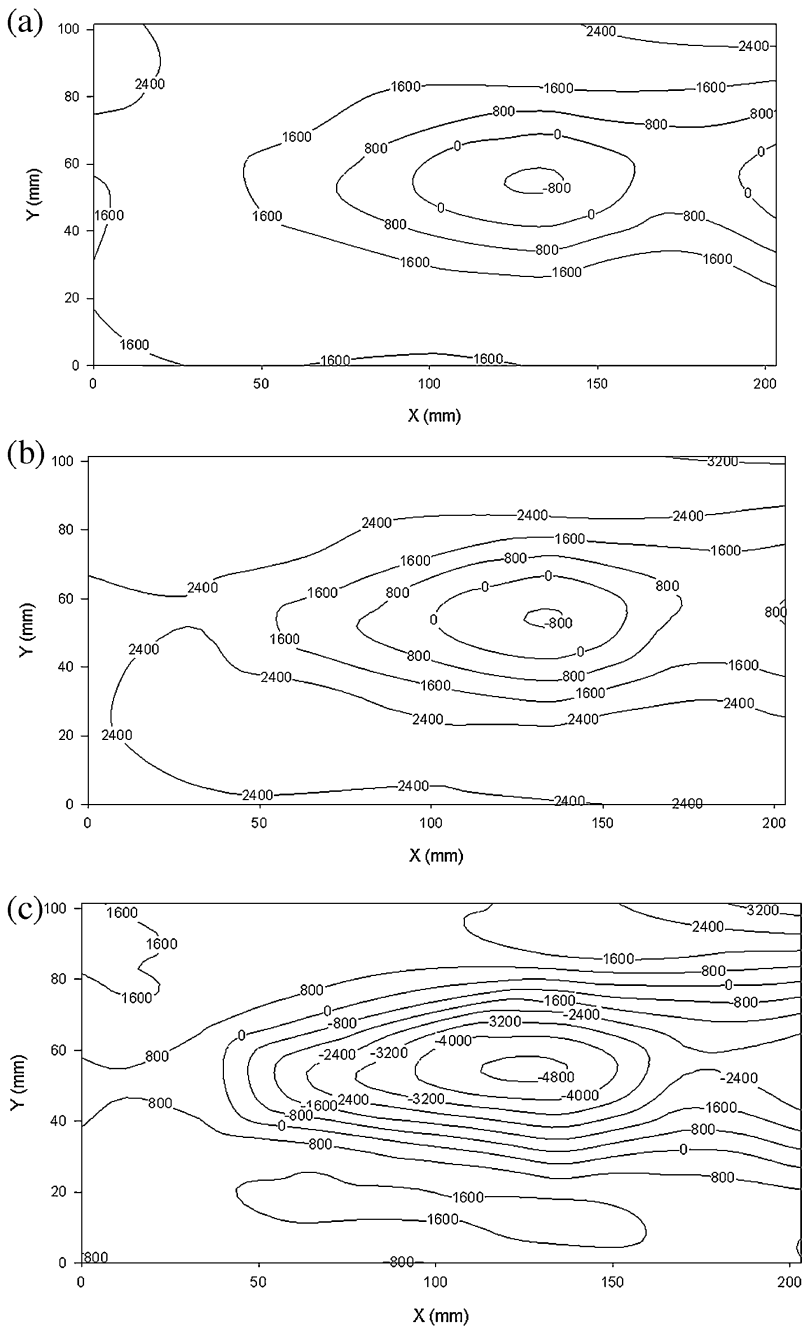

Fig. 6. Heat flux vector contours at $Re = 18{,}000$: (a) reference case (without obstacle), (b) cubic obstacle and (c) delta-wing obstacle.

5. Conclusions

In this study, the delta-wing and the cubic obstacle were used as vortex generators, and their wake effects on thermal mixing in liquid metal ($Ga_{67}In_{20.5}Sn_{12.5}$) free-surface flow were investigated by using LMX at PPPL. In order to understand the thermal mixing induced by these obstacles, the liquid metal free-surface flow in the channel without magnetic fields was partially heated and the temperature distributions on the channel bottom were measured. The results of these experiments can be summarized as follows:

(1) Based on the comparison of the temperature contours, we conclude that the delta-wing obstacle transports the high temperature fluid heated at the free-surface to the bottom wall more efficiently than the cubic obstacle and the reference case.
(2) Based on the comparison of heat flux contours and the maximum heat flux points, it is found that the obstacle enhanced the thermal mixing of the fluid, and the delta-wing obstacle allows the faster mixing of the higher temperature fluid from the free-surface to the wall compared to the cubic obstacle.

This study allows a deeper understanding of the localized high heat flux from the wall of the free-surface flow by using different obstacles and it is possible to remove the high heat flux locally from the wall.

Based on these results, an upgrade to LMX or a similar machine by impinging installing jets on the backside of the wall to remove

the localized heat flux should be considered. This would help removal of the localized high heat flux from the wall of the free-surface flow by using the delta-wing obstacles.

Acknowledgment

Mr. Koji Kusumi greatly appreciates the support of the Atomic Energy Society of Japan for supporting his travel expenses from Japan to USA and back.

References

[1] M.A. Abdou, et al., On the exploration of innovative concepts for fusion chamber technology, Fusion Eng. Des. 54 (2001) 181–247.
[2] T. Kunugi, et al., A new cooling concept of free-surface flow balanced with surface tension for FFHR, Fusion Eng. Des. 65 (2003) 381–385.
[3] T. Kunugi, et al., Investigation of cascade-type falling liquid-film along first wall of laser-fusion reactor, Fusion Eng. Des. 83 (2008) 1888–1892.
[4] S.V. Mirnov, et al., Liquid–metal tokamak divertors, J. Nucl. Mater. 196–198 (1992) 45–49.
[5] M.A. Jaworski, et al., Thermoelectric magnetohydrodynamic stirring of liquid metals, Phys. Rev. Lett. 104 (9) (2010) 094503.
[6] J.R. Rhoads, et al., Effects of magnetic field on the turbulent wake of a cylinder in free-surface mganetohydrodynamics channel flow, J. Fluid Mech. 742 (2014) 446–465.
[7] B. Mück, Three-dimensional MHD flows in rectangular channels with internal obstacles, J. Fluid Mech. 418 (2000) 265–295.
[8] D. Chatterjee, S.K. Gupta, MHD flow and heat transfer behind a square cylinder in a channel under strong axial magnetic field, Int. J. Heat Mass Transfer 88 (2015) 1–13.
[9] H. Huang, B. Li, Heat transfer enhancement of free-surface MHD-flow by a protrusion wall, Fusion Eng. Des. 85 (2010) 1496–1520.
[10] M.C. Gentry, A.M. Jacobi, Heat transfer enhancement by delta-wing-generated tip vortices in flat-plate and developing channel flow, J. Heat Transfer 124 (2002) 1158–1168.
[11] A. Joardar, A.M. Jacobi, Impact of leading edge delta-wing vortex generators on the thermal performance of a flat tube, louvered-fin compact heat exchanger, Int. J. Heat Mass Transfer 48 (2005) 1480–1493.
[12] N.B. Morley, et al., GaInSn usage in the research laboratory, Rev. Sci. Instrum. 79 (2008) 056107.